Gomez-Lamarca et al., http://www.jcb.org/cgi/content/full/jcb.201411001/DC1

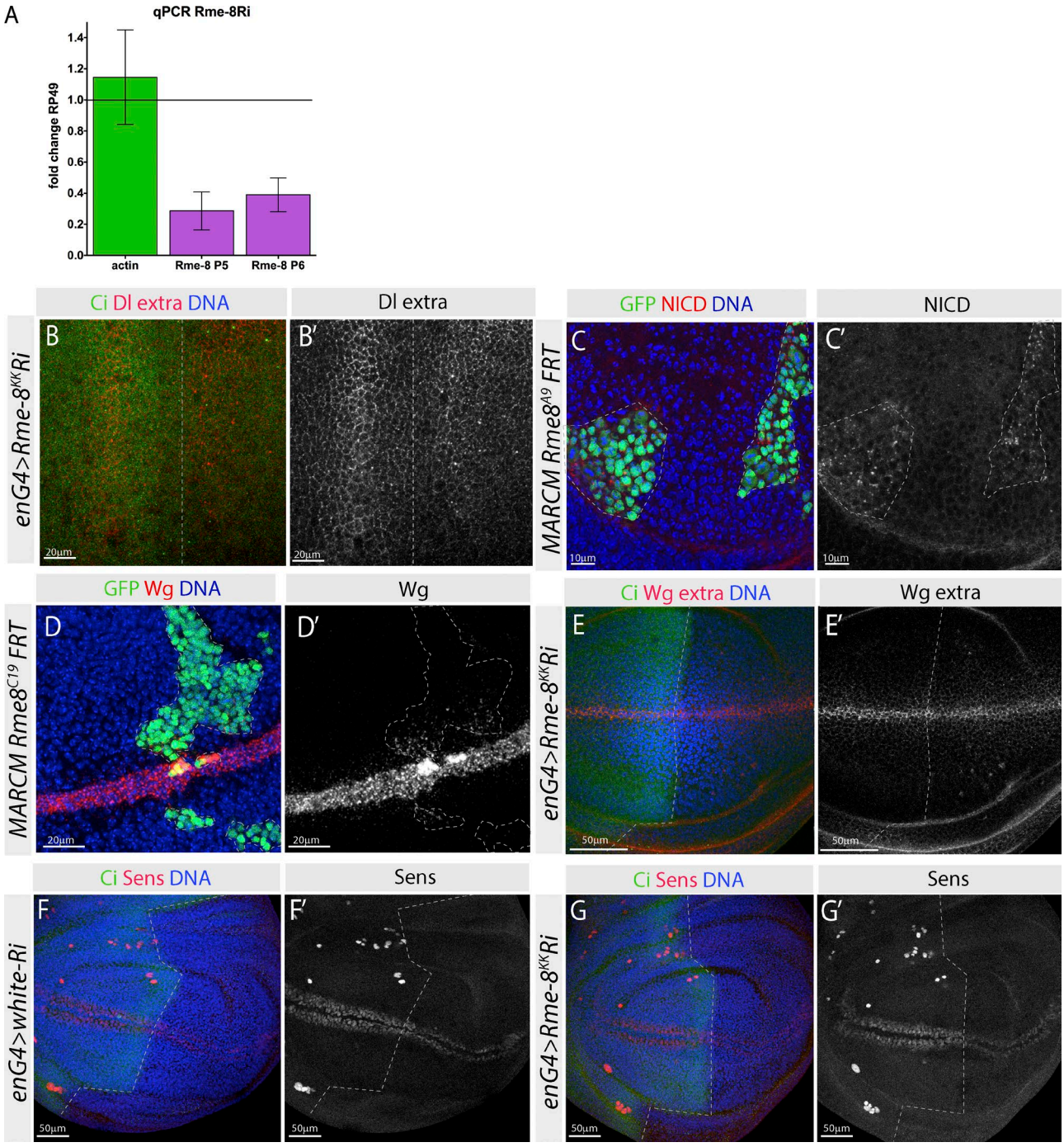

Figure S1. ***Rme-8 Ri* knockdown and phenotypes.** (A) Graph showing reduction of *Rme-8* mRNA levels respect to those of a highly expressed gene, *actin*, measured by quantitative PCR (qPCR) using two pairs of primers that target different regions of the gene. Bars indicate SEM. Horizontal line indicates fold change = 1 (expected result if RNA levels were unaffected). (B and B′) Wing imaginal disc stained for Ci, Dl extracellular (red in B; white in B′) and Hoechst (blue), shows reduction of Dl membrane levels in *Rme-8* knockdown cells (right from dotted line). (C and C′) *Rme-8*^{A9} mutant clones (green, outlined by the dotted lines) generated by MARCM system show accumulation of intracellular Notch (red in C; white in C′). (D and D′) *Rme-8*^{C19} mutant clones (green, outlined by the dotted lines) generated by MARCM system show accumulation of intracellular Wg (red in C; white in C′) both inside the receiving cells far from the source of Wg secretion and, to a lesser extent, inside the producing cells. (E and E′) Wing imaginal disc stained for Ci, Wg extracellular (red in E; white in E′) and Hoechst (blue), shows no difference in Wg extracellular levels in *Rme-8* knockdown cells (right from dotted line). (F–G′) Wing imaginal discs stained for Ci, Senseless (red in F and G; white in F′ and G′), and Hoechst (blue) show no change in Senseless levels of expression in *Rme-8* knockdown cells (right from dotted line in G) compared with WT (*white-Ri*, right from dotted line in F).

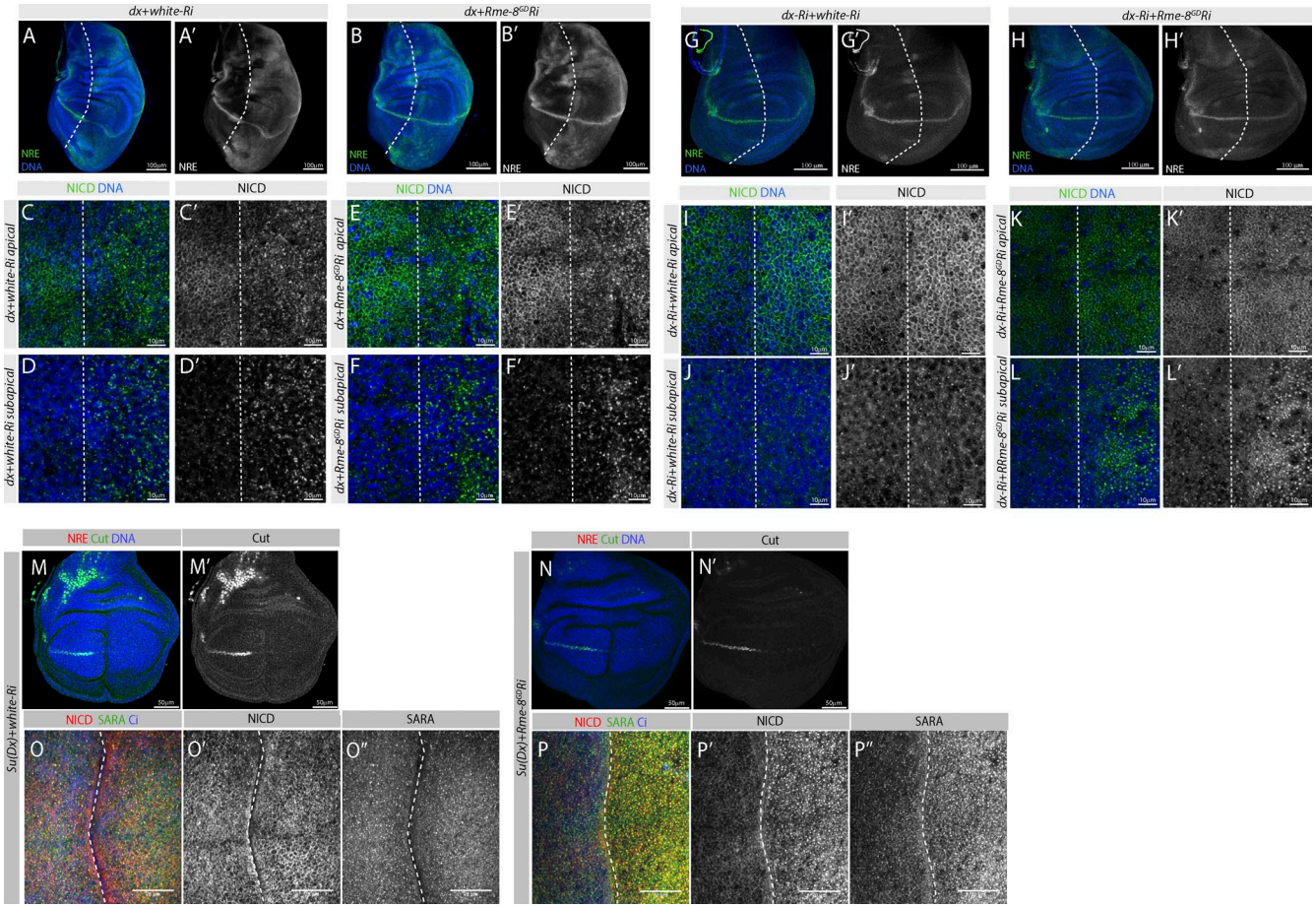

Figure S2. **Rme-8 appears regulate Notch trafficking independently of Dx and Su(dx).** (A–B′) NRE-GFP expression (green in A and B; white in A′ and B′) is detected throughout the domain of Dx overexpression (A, right of dotted line) and is not rescued by depletion of *Rme-8* (B, right of dotted line). (C–F′) Notch (green, in C–F; white in C′–F′) is depleted from the apical membrane and accumulates intracellularly in both *dx*-expressing (C and D, respectively) and *dx+Rme8-Ri*–expressing cells (E and F, respectively). Images are from third-instar wing discs expressing either *dx+white-Ri* (A, C, and D) or *dx+Rme8-Ri* (B, E, and F) in the posterior compartment (right of dashed lines). (G–H′) NRE-GFP expression (green in G and H; white in G′ and H′) is still expressed at the D/V boundary when dx is depleted (G, right of dotted line) but is detectably reduced when *Rme-8* is also knocked down (H, right of dotted line). (I–L′) Notch (green in I–L; white in I′–L′) accumulates at the apical membrane in both *dx-Ri*–expressing (I and J) and *dx-Ri+Rme8-Ri*–expressing cells (K and L) but in subapical endosomes only in *dx-Ri+Rme8-Ri*–expressing cells (K and L). Images are from third-instar wing discs expressing either *dx-Ri +white-Ri* (G, I, and J) or *dx-Ri +Rme8-Ri* (H, K, and L) in the posterior compartment (right of dashed lines). (M–N′) Cut expression (red in M and N; white in M′ and N′) is depleted at the D/V boundary when Su(dx) is overexpressed alone (M, right of dotted line) or in combination with *Rme-8* knockdown (N, right of dotted line). (O–P″) Distribution of NICD (red in O and P; white in O′ and P′), SARA (green M and N; white in O″ and P″) and Ci from wing discs expressing *Su(dx)+white-Ri* (O) or *Su(dx)+Rme-8-Ri* (P), showing that *Rme-8* does not modified *Su(dx)* phenotype.

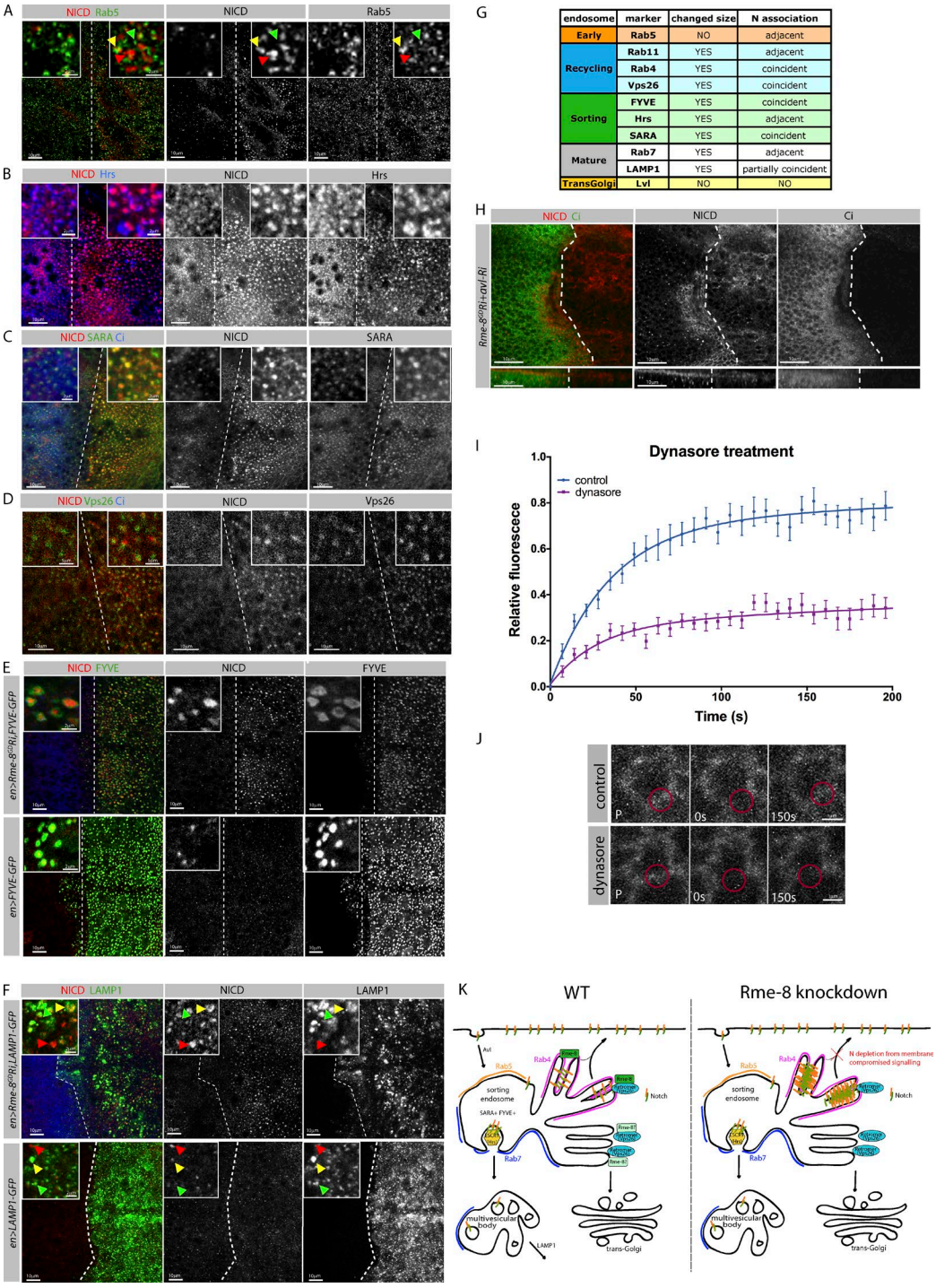

Figure S3. **Notch associates with enlarged endosomes.** (A–D) Relationship between Notch (NICD) and endocytic proteins in wing discs expressing *Rme8-Ri* in the posterior compartment (right side of dashed line). (A) Enlarged puncta containing NICD but not Rab5 are detected in the *Rme-8*–depleted cells, NICD appears to accumulate away from Rab5 (see insets). (B) Enlarged puncta containing NICD and Hrs are detected in the *Rme-8*–depleted cells, NICD appears to accumulate beside Hrs (see insets). (C) Enlarged puncta containing NICD and SARA are detected in the *Rme-8* depleted cells; NICD appears to colocalize with SARA (see insets). (D) Enlarged puncta containing NICD and Vps26 are detected in the *Rme-8*–depleted cells; NICD colocalizes with Vps26 (see insets). (E) Enlarged NICD puncta appear surrounded by FYVE. Similar relationship is detected in WT tissues, where the puncta are smaller; FYVE-GFP expression alone does substantially alter the Notch accumulations (insets). (F) Enlarged puncta containing NICD and LAMP1 are detected in the *Rme-8*–depleted cells. Some puncta contain both proteins (insets, yellow arrowheads) others contain LAMP1 only (insets, green arrowheads), or NICD only (insets, red arrowheads). LAMP1 distribution is also disrupted in comparison to controls (bottom). Expression of LAMP1-GFP alone does not lead to altered accumulation of NICD. (G) Summary table with relevant information about the endosomal markers analyzed in *Rme-8* depleted cells. (H) *Avl* knockdown suppresses Notch accumulation in *Rme-8*–depleted cells. Distribution of NICD (left, red; right, white) and Ci (left, green; right, white) from wing discs expressing *avl-Ri+Rme-8-Ri*; xy section of discs at the subapical plane (top) and xz cross sections of the same specimens (bottom). (I and J) FRAP experiments, measuring recovery of Notch-GFP after photobleaching. (I) Plot of averaged recovery curves (mean ± SEM) from Notch-GFP FRAP experiments with best-fit curves as solid lines of WT and dynasore-treated discs. (J) Single FRAP examples with red circles showing the bleach spots. P, prebleach. (K) Proposed model of Rme-8 function in WT and subsequent *n* trafficking changes in Rme-8–depleted conditions.

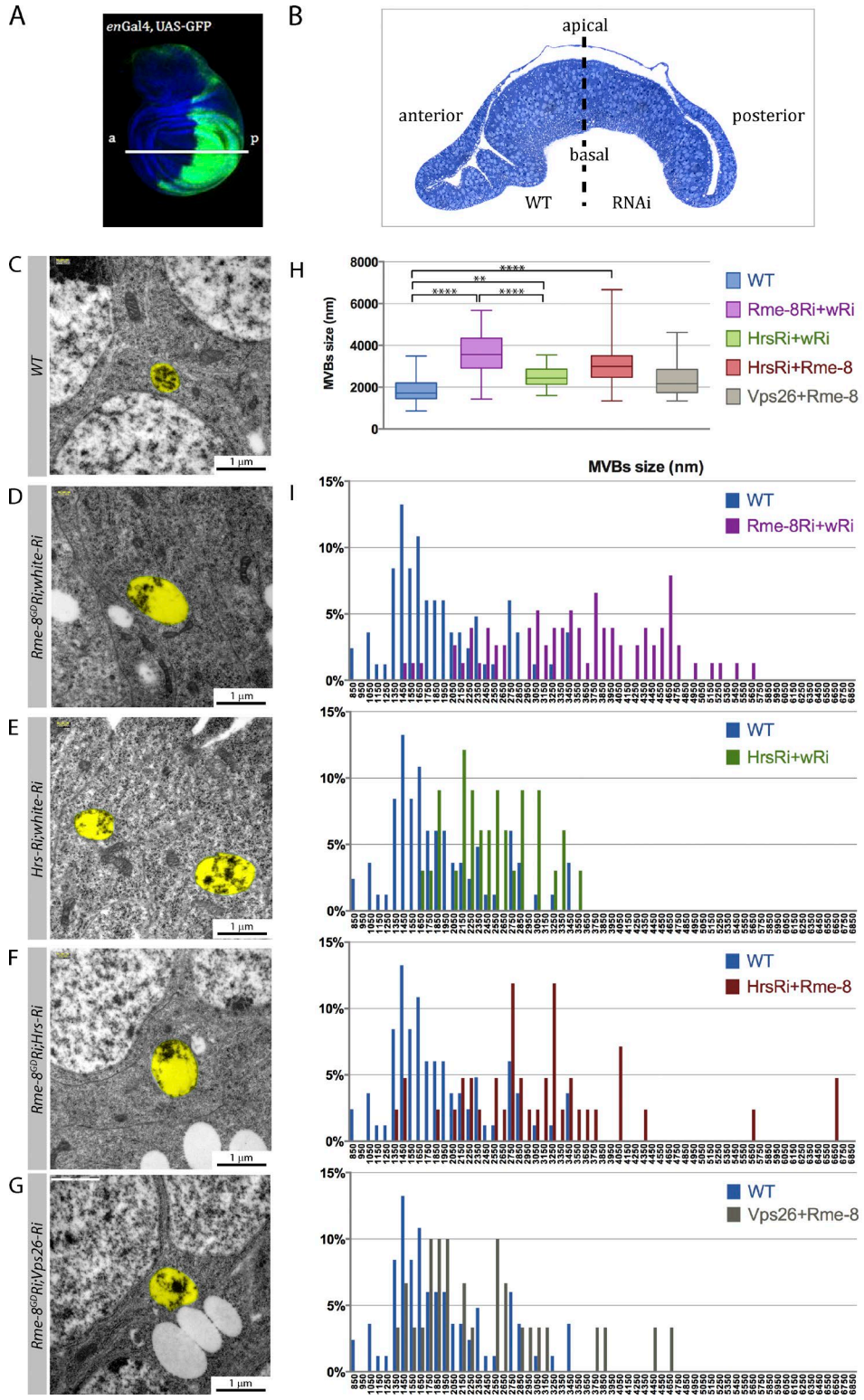

Figure S4. **TEM analysis of *Rme-8*, *Hrs*, and *Vps26* knockdowns.** (A) Wing disc stained for Hoechst (blue), showing the expression pattern of *en-Gal4* revealed by *UAS-GFP* (green), which was used to express different *UAS Ri*. The discs were sectioned at the level of the white line. a, anterior; p, posterior (B) Semi–cross section at the level indicated by the white line in A. Phenotypes of the posterior cells were compared with the anterior WT cells. (C–G) Representative MVBs highlighted in pseudocolor (yellow) of anterior WT (C), posterior *Rme-8*–depleted (D), *Hrs*-depleted (E), *Rme-8+Hrs*–depleted (F), and *Rme-8+Vps26*–depleted (G) cells. The MVBs of all knockdown conditions are enlarged compared with the control, except those of the *Rme-8+Vps26* double knockdown. (H) Box plot and statistical analysis of the perimeter of the MVBs. All measurements from anterior compartment MVBs in the four knockdown experiments were included in the WT group for the statistical analysis. Asterisks indicate statistical differences. **, P = 0.01–0.001; ****, P < 0.0001). WT *n* = 83, *Rme-8-Ri;w-Ri n* = 76, *Hrs-Ri;w-Ri n* = 33, *Hrs-Ri;Rme-8-Ri n* = 42, and *Vps26-Ri;Rme-8-Ri n* = 30. Box plots show boxes from 25th to 75th percentiles, whiskers represent maximum and minimum values in the dataset, and lines show the median values. (I) Frequency distribution plots of MVB sizes for each condition.

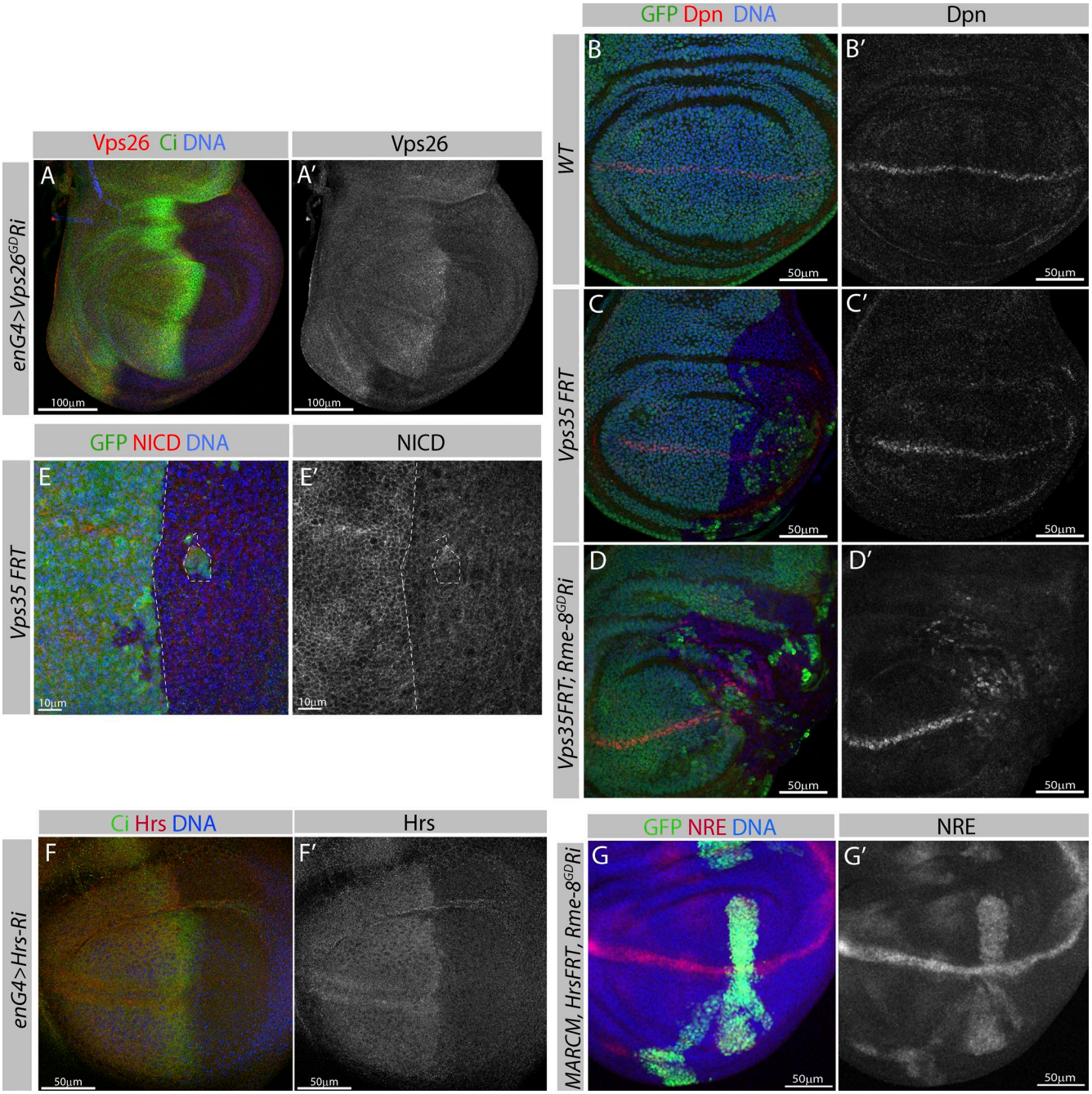

Figure S5. **Retromer and ESCRT-0 Ri validation and phenotypes.** (A and A′) Wing disc stained for Hoechst, Ci, and Vps26 to show the knockdown effect of the *Vps26-Ri* line using *en-Gal4* to direct its expression. (B–D′) Wing discs stained for Hoechst and GFP. Dpn expression (red in B–D; white in B′–D′) is up-regulated in *Vps35* mutant clones (absence of GFP) expressing *Rme-8Ri* under *hh-Gal4* control (D) compared with WT (A) or *Vps35* mutant alone (B). (E and E′) Wing discs stained for Hoechst (blue) and GFP. Membrane levels of Notch (red) are reduced in *Vps35* mutant clones (absence of GFP). (F and F′) Wing disc stained for Hoechst (blue), Ci, and Hrs to show the knockdown effect of the *Hrs-Ri* line using *en-Gal4* to direct its expression. (G and G′) NRE-mCherry expression (red in G; white in G′) is up-regulated autonomously in *Hrs* mutant clones (GFP$^+$) expressing *Rme-8Ri*.

Table S1. **Details of *Drosophila* strains**

Strains	Summary	Reference
Rme-8 Ri GD	322 bp hairpin against exon 7	VDRC 22671
Rme-8-Ri KK	768 bp hairpin against exon7	VDRC 107706
w-Ri	21 bp hairpin against exon 4	BL 35573
Su(H)-Ri	431 bp hairpin against exon 3	BL 28900
Dx-Ri GD	338 bp hairpin against exon 1	VDRC 7795
Dx-Ri KK	301 bp hairpin against exon 2	VDRC 106086
Vps26-Ri	321 bp hairpin against exon 2	VDRC 18396
Vps26-Ri	21 bp hairpin against exon 2	BL 38937
Hrs-Ri	21 bp hairpin against exon 4	BL 33900
Hrs-Ri	21 bp hairpin against exon 4	BL 34086
Stam-Ri	361 bp hairpin against exon 3	VDRC 22497
KuzDN	Dominant-negative construct expressing a version of Kux lacking the metalloprotease domain	BL 6578; Pan and Rubin, 1997
UAS-Dx	Full-length Deltex cloned in pUAST plasmid	Matsuno et al., 2002
UAS-Su(dx)	Full open reading frame of Su(dx) inserted into the pUAST vector	Cornell et al., 1999
SalEPv-Gal4	1,080 bp fragment from the sal enhancer (salEPv) clones into pW8-Gal4	Cruz et al., 2009
Rme-8 C19	X-ray mutagenesis	Chang et al., 2004
Rme-8 A9	X-ray mutagenesis	Chang et al., 2004
Vps35 MH20	A 2-kb deletion that removes the first three exons including the translation start site obtained by *P* element imprecise excision	Franch-Marro et al., 2008
Hrs D28	Nonsense mutation at amino acid Q270	Lloyd et al., 2002
NRE-Cherry	Three copies of Gbe palindromic binding site plus the Su(H) binding sites from the E(Spl) m8 gene, upstream of the hsp70 minimal promoter controlling the expression of mCherry inserted using the FC31 system	Housden et al., 2012
NRE-GFP	Three copies of Gbe palindromic binding site plus the Su(H) binding sites from the E(Spl) m8 gene, upstream of the hsp70 minimal promoter controlling the expression of EGFP inserted using the FC31 system	Housden et al., 2012
Tub-Rab4-mCherry	Construct generated by slice over extension PCR from EST-clone RE40706 (DGRC) and mCherry-cDNA (pAB118-mCherry) and cloned into pCasp-tubPromoter-3′UTR	Yousefian et al., 2013
UAS-GFP-myc-2xFYVE	Two FYVE fingers from Hrs (aa 147–223) separated by the linker QGQGA and tagged with a myc and EGFP epitope in the N terminus cloned into pUAST vector	Wucherpfennig et al., 2003
UAS-Lamp1-GFP	Cleavable preprolactin signal sequenced followed by EGFP and a transmembrane domain and cytoplasmic tail derived from human LAMP1 cloned into the pUAST vector	BL 42714; Pulipparacharuvil et al., 2005
Notch-GFP	Rescue construct containing 44,868 nucleotides from −6.233 nucleotides upstream the transcription start site to 1,245 nucleotides downstream of the 3′UTR cloned into attb-P(acman)-ApR vector and a GFP inserted in intracellular domain of Notch (aa 2,388)	Couturier et al., 2013

DGRC, Drosophila Genomics Resource Center; BL, Bloomington Stock Center; VDRC, Vienna Drosophila Resource Center.

Table S2. **Details of primary antibodies**

Antibody	Dilution	Antigen	Reference
Mo NICD	1:20	Intracellular domain of *Drosophila* Notch, amino acids 1,791–2,504	C17.9C6 DSHB; Fehon et al., 1990
Mo NECD	1:20	EGF repeats 12–20 of the extracellular domain of *Drosophila* Notch	C458.2H DSHB; Diederich et al., 1994
Rat NECD	1:500	Extracellular domain of *Drosophila* Notch	Fehon et al., 1990
Mo Wg	1:20	Wg amino acids 3–468 fused to TrpE	4E4 DSHB; van den Heuvel et al., 1989
GP Dl	1:3,000	EGF-like repeats 4–9, amino acids 350–529, of *Drosophila* Dl fused to β-galactosides	Huppert et al., 1997
Rat Ci	1:20	amino acids 700–850 (C terminus of the Zn finger domain) of Ci fused to GST	2A1 DSHB; Motzny and Holmgren, 1995
Rb GFP	1:1,000	Polyclonal against GFP isolated directly from jellyfish *Aequorea victoria*	A6455 Invitrogen
Rb dsRed	1:200	Polyclonal	632496 Takara Bio Inc.
Rb Rab7	1:3,000	Synthetic peptide CNDFPDQITLGSQNNRPG, amino acid residues 184–200 of *Drosophila* Rab7	Tanaka and Nakamura, 2008
Rb Rab11	1:8,000	Synthetic peptide CSQKQIRDPPEGDVI, amino acid residues 177–191 of *Drosophila* Rab11	Tanaka and Nakamura, 2008
Rb Rab5	1:500	Synthetic peptide covering amino acids 200 to C terminus of Rab5 fused to KLH	31261 Abcam
GP Hrs	1:1,000	N-terminal domain of HRS fused to GST	Lloyd et al., 2002
Rb Lva	1:500	Fragment close to the C terminus domain of Lavalamp fused to GST	Sisson et al., 2000
Rb Avl	1:1,000	Peptide covering amino acids 1–258 from *avl* cDNA fused to GST	Lu and Bilder, 2005
Rb SARA	1:500	C-terminal 174 amino acids fused to GST	Coumailleau et al., 2009
GP Vps26	1:1,000	Full-length Vps26 protein fused to Hisx6	Wang et al., 2014

Mo, mouse; GP, guinea pig; Rb, rabbit.

Table S3. **Details of secondary antibodies**

Antibody	Specificity	Catalog number
Donkey anti–Mo FITC	AffiniPure donkey anti–Mo IgG (H+L)	715-095-151 Jackson ImmunoResearch Laboratories, Inc.
Donkey anti–Mo Cy3	AffiniPure donkey anti–Mo IgG (H+L)	715-165-151 Jackson ImmunoResearch Laboratories, Inc.
Donkey anti–Mo Cy5	AffiniPure donkey anti–Mo IgG (H+L)	715-175-151 Jackson ImmunoResearch Laboratories, Inc.
Donkey anti–Mo 488	Donkey anti–Mo IgG (H+L)	A21202 Invitrogen
Donkey anti–Rb FITC	AffiniPure donkey anti–Rb IgG (H+L)	711-095-152 Jackson ImmunoResearch Laboratories, Inc.
Goat anti–Rb Cy3	AffiniPure goat anti–Rb IgG (H+L)	111-165-144 Jackson ImmunoResearch Laboratories, Inc.
Donkey anti–Rb Cy5	AffiniPure donkey anti–Rb IgG (H+L)	711-175-152 Jackson ImmunoResearch Laboratories, Inc.
Donkey anti–Rb 568	Donkey anti–Rb IgG (H+L)	A10042 Invitrogen
Donkey anti–rat FITC	AffiniPure donkey anti–rat IgG (H+L)	712-095-153 Jackson ImmunoResearch Laboratories, Inc.
Donkey anti–rat Cy3	AffiniPure donkey anti–rat IgG (H+L)	712-165-153 Jackson ImmunoResearch Laboratories, Inc.
Donkey anti–rat Cy5	AffiniPure donkey anti–rat IgG (H+L)	712-175-153 Jackson ImmunoResearch Laboratories, Inc.
Donkey anti–GP FITC	AffiniPure donkey anti–GP IgG (H+L)	706-095-148 Jackson ImmunoResearch Laboratories, Inc.
Donkey anti–GP Cy3	AffiniPure donkey anti–GP IgG (H+L)	706-165-148 Jackson ImmunoResearch Laboratories, Inc.

Mo, mouse; GP, guinea pig; Rb, rabbit; H+L, heavy and light chain.

References

Chang, H.C., M. Hull, and I. Mellman. 2004. The J-domain protein Rme-8 interacts with Hsc70 to control clathrin-dependent endocytosis in *Drosophila*. *J. Cell Biol.* 164:1055–1064. http://dx.doi.org/10.1083/jcb.200311084

Cornell, M., D.A. Evans, R. Mann, M. Fostier, M. Flasza, M. Monthatong, S. Artavanis-Tsakonas, and M. Baron. 1999. The *Drosophila melanogaster* Suppressor of deltex gene, a regulator of the Notch receptor signaling pathway, is an E3 class ubiquitin ligase. *Genetics.* 152:567–576.

Coumailleau, F., M. Fürthauer, J.A. Knoblich, and M. González-Gaitán. 2009. Directional Delta and Notch trafficking in Sara endosomes during asymmetric cell division. *Nature.* 458:1051–1055. http://dx.doi.org/10.1038/nature07854

Couturier, L., K. Mazouni, and F. Schweisguth. 2013. Numb localizes at endosomes and controls the endosomal sorting of notch after asymmetric division in *Drosophila*. *Curr. Biol.* 23:588–593. http://dx.doi.org/10.1016/j.cub.2013.03.002

Cruz, C., A. Glavic, M. Casado, and J.F. de Celis. 2009. A gain-of-function screen identifying genes required for growth and pattern formation of the *Drosophila melanogaster* wing. *Genetics.* 183:1005–1026. http://dx.doi.org/10.1534/genetics.109.107748

Diederich, R.J., K. Matsuno, H. Hing, and S. Artavanis-Tsakonas. 1994. Cytosolic interaction between deltex and Notch ankyrin repeats implicates deltex in the Notch signaling pathway. *Development.* 120:473–481.

Fehon, R.G., P.J. Kooh, I. Rebay, C.L. Regan, T. Xu, M.A.T. Muskavitch, and S. Artavanis-Tsakonas. 1990. Molecular interactions between the protein products of the neurogenic loci Notch and Delta, two EGF-homologous genes in *Drosophila*. *Cell.* 61:523–534. http://dx.doi.org/10.1016/0092-8674(90)90534-L

Franch-Marro, X., F. Wendler, S. Guidato, J. Griffith, A. Baena-Lopez, N. Itasaki, M.M. Maurice, and J.-P. Vincent. 2008. Wingless secretion requires endosome-to-Golgi retrieval of Wntless/Evi/Sprinter by the retromer complex. *Nat. Cell Biol.* 10:170–177. http://dx.doi.org/10.1038/ncb1678

Housden, B.E., K. Millen, and S.J. Bray. 2012. *Drosophila* reporter vectors compatible with ΦC31 integrase transgenesis techniques and their use to generate new Notch reporter fly lines. *G3 (Bethesda).* 2:79–82. http://dx.doi.org/10.1534/g3.111.001321

Huppert, S.S., T.L. Jacobsen, and M.A. Muskavitch. 1997. Feedback regulation is central to Delta-Notch signalling required for *Drosophila* wing vein morphogenesis. *Development.* 124:3283–3291.

Lloyd, T.E., R. Atkinson, M.N. Wu, Y. Zhou, G. Pennetta, and H.J. Bellen. 2002. Hrs regulates endosome membrane invagination and tyrosine kinase receptor signaling in *Drosophila*. *Cell.* 108:261–269. http://dx.doi.org/10.1016/S0092-8674(02)00611-6

Lu, H., and D. Bilder. 2005. Endocytic control of epithelial polarity and proliferation in *Drosophila*. *Nat. Cell Biol.* 7:1232–1239. http://dx.doi.org/10.1038/ncb1324

Matsuno, K., M. Ito, K. Hori, F. Miyashita, S. Suzuki, N. Kishi, S. Artavanis-Tsakonas, and H. Okano. 2002. Involvement of a proline-rich motif and RING-H2 finger of Deltex in the regulation of Notch signaling. *Development.* 129:1049–1059.

Motzny, C.K., and R. Holmgren. 1995. The *Drosophila* cubitus interruptus protein and its role in the wingless and hedgehog signal transduction pathways. *Mech. Dev.* 52:137–150. http://dx.doi.org/10.1016/0925-4773(95)00397-J

Pan, D., and G.M. Rubin. 1997. Kuzbanian controls proteolytic processing of Notch and mediates lateral inhibition during *Drosophila* and vertebrate neurogenesis. *Cell.* 90:271–280. http://dx.doi.org/10.1016/S0092-8674(00)80335-9

Pulipparacharuvil, S., M.A. Akbar, S. Ray, E.A. Sevrioukov, A.S. Haberman, J. Rohrer, and H. Krämer. 2005. *Drosophila* Vps16A is required for trafficking to lysosomes and biogenesis of pigment granules. *J. Cell Sci.* 118:3663–3673. http://dx.doi.org/10.1242/jcs.02502

Sisson, J.C., C. Field, R. Ventura, A. Royou, and W. Sullivan. 2000. Lava lamp, a novel peripheral golgi protein, is required for *Drosophila melanogaster* cellularization. *J. Cell Biol.* 151:905–918. http://dx.doi.org/10.1083/jcb.151.4.905

Tanaka, T., and A. Nakamura. 2008. The endocytic pathway acts downstream of Oskar in *Drosophila* germ plasm assembly. *Development.* 135:1107–1117. http://dx.doi.org/10.1242/dev.017293

van den Heuvel, M., R. Nusse, P. Johnston, and P.A. Lawrence. 1989. Distribution of the wingless gene product in *Drosophila* embryos: a protein involved in cell-cell communication. *Cell.* 59:739–749. http://dx.doi.org/10.1016/0092-8674(89)90020-2

Wang, S., K.L. Tan, M.A. Agosto, B. Xiong, S. Yamamoto, H. Sandoval, M. Jaiswal, V. Bayat, K. Zhang, W.-L. Charng, et al. 2014. The retromer complex is required for rhodopsin recycling and its loss leads to photoreceptor degeneration. *PLoS Biol.* 12:e1001847. http://dx.doi.org/10.1371/journal.pbio.1001847

Wucherpfennig, T., M. Wilsch-Bräuninger, and M. González-Gaitán. 2003. Role of *Drosophila* Rab5 during endosomal trafficking at the synapse and evoked neurotransmitter release. *J. Cell Biol.* 161:609–624. http://dx.doi.org/10.1083/jcb.200211087

Yousefian, J., T. Troost, F. Grawe, T. Sasamura, M. Fortini, and T. Klein. 2013. Dmon1 controls recruitment of Rab7 to maturing endosomes in *Drosophila. J. Cell Sci.* 126:1583–1594. http://dx.doi.org/10.1242/jcs.114934